

Microwave Spectrum for Bromo(sulphido)boron, BrBS

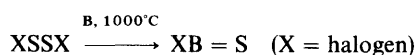
Terrence A. Cooper, Steven Firth and Harold W. Kroto

School of Chemistry and Molecular Sciences, University of Sussex, Brighton BN1 9QJ, UK

The rotational spectrum of the transient molecule bromo(sulphido)boron, $\text{BrB}=\text{S}$, has been observed. The molecule was produced by the high-temperature reaction between gaseous dibromo disulphide, Br_2S_2 , and crystalline boron chips at *ca.* 1000 °C, and was studied by microwave spectroscopy between 26.5 and 40 GHz. The spectrum is that of a linear molecule. Ground-state rotation, distortion and quadrupole coupling constants have been obtained for 10 of the 12 isotopic variants in natural abundance. A wealth of spectroscopic data has been obtained which has allowed an extremely detailed structure analysis to be performed. The resulting bond lengths are $r_s(\text{BrB}) = 1.831(2)$ Å and $r_s(\text{B}=\text{S}) = 1.608(2)$ Å. Transitions due to vibrationally excited states have also been measured and analysed to yield a range of vibration-rotation parameters.

The sulphidoborons are an interesting class of linear molecules which are isoelectronic with the phosphalkynes and isovalent with the nitriles. They are unstable with respect to polymerization, and have a half-life at low pressures of the order of a few seconds. The 'parent' compound, HBS, was first detected mass-spectrometrically in the products of reaction between hydrogen sulphide and crystalline boron at *ca.* 1000 °C by Kirk and Timms in 1967.¹ Since then, microwave,^{2,3} photoelectron^{4,5} and infrared⁶ techniques have been used to determine its structural and other molecular parameters. An equilibrium structure has been deduced by Mills and Turner.⁷

In a general programme aimed at the study of unstable molecules (phosphalkynes, phosphalkenes, sulphidoborons and selenidoborons⁸), routes to the substituted analogues were developed using substituted disulphides as precursors. The first substituted species, MeBS was detected by microwave spectroscopy in the products of thermolysis of MeSSMe over crystalline boron at 850 °C.^{9,10} The molecule is a symmetric top and has a readily identifiable microwave spectral pattern; its structure was confirmed by measurements on the species $\text{Me}^{10}\text{B}^{32}\text{S}$ and $\text{Me}^{11}\text{B}^{34}\text{S}$. These experiments led naturally to the study of the halides by essentially the same reaction,



The first halide studied this way was the chloride, CIBS,¹¹ for which a wide variety of isotopic species was studied to obtain accurate structural information. The photoelectron spectrum of this species has also been recorded.¹²

This work was then extended to the detection of FBS by microwave and photoelectron spectroscopies.^{8,13} An accurate structure was determined from the substitution coordinates of the boron and sulphur atoms and the first- and second-moment equations.

The work described here is a further extension of the above project to generate and record the microwave spectrum of BrBS. The observed spectrum is consistent with that of a linear triatomic molecule. Transitions belonging to the 10 most abundant of the 12 possible isotopic species have been observed in natural abundance and analysed. This wealth of data allows the possibility of several routes to the determination of the bond lengths, and allows a realistic assessment of the reliability of these routes to be made.

Experimental

BrSSBr was prepared by sealing stoichiometric amounts of bromine and flowers of sulphur in an ampoule, and heating

the mixture to 200 °C in an oven. The resulting dark-red liquid was used without further purification. BrSSBr vapour was then passed over crystalline boron chips (Koch-Light) heated to *ca.* 1000 °C in a quartz tube. Br_2S_2 was sufficiently involatile that pressures of 60 mTorr could be obtained by fully opening the ampoule tap with the sample at room temperature. The quartz tube (8 mm i.d.) was loosely packed for *ca.* 20 cm of its length with boron, and heated over this length by a small resistance furnace. The reaction products were then passed directly into the microwave cell.

When recording survey scans, pressures of 60 mTorr were used, with the Br_2S_2 at room temperature. On terminating the Br_2S_2 flow, the cell pressure dropped to 2-5 mTorr above background, this pressure being due to bromo(sulphido)boron being pumped off the boron surface. These conditions were used to record high-resolution spectra. Vibrational satellite spectra were recorded with the microwave cell at room temperature, ground-state spectra were recorded with the cell cooled to dry-ice temperature.

All spectra were recorded on a Hewlett-Packard 8460A spectrometer, operating between 26.5 and 40 GHz.

Spectrum and Analysis

The observed spectrum of the products of the high-temperature reaction between BrSSBr and boron between 26.5 and 40 GHz shows three equally spaced groups of $\Delta J = +1$ transitions of BrBS, and the $J = 1 \leftarrow 0$ transition of HBS, which is also formed in the reaction.

A medium-resolution scan of the $J = 9 \leftarrow 8$ transition is given in Fig. 1, presented so that the most intense peaks, due to ground-state transitions of $^{81}\text{Br}^{11}\text{B}^{32}\text{S}$ and $^{79}\text{Br}^{11}\text{B}^{32}\text{S}$, are vertically aligned. The boron isotope shift shows up clearly in this spectrum, but transitions due to ^{33}S and ^{34}S are off scale. The observed relative intensities are consistent with this isotopic assignment. The gradual decrease in intensity across the spectrum from low to high frequencies is due to sample variation during the scan. The small magnitude of the boron shift identifies it as the central atom in this molecule.

The ground-state transition of each species has two associated vibrational sequences. The third, belonging to the $\text{B}=\text{S}$ stretch, is too weak to be identified. The degenerate bending vibration, ν_2 , extends to higher frequencies and exhibits *l*-type splitting. The other progressions belongs to ν_3 , the $\text{Br}-\text{B}$ stretch, extends to low frequencies and shows similar Stark structure to the ground-state lines. Transitions due to molecules in excited combination levels are also seen, and identified in Fig. 1.

Table 1 Ground-state frequencies (MHz) and assignments for BrBS

<i>J</i>	ΔF	<i>F</i> "	[1] (79, 11, 32)		[2] (79, 11, 33)		[3] (79, 11, 34)		[4] (79, 10, 32)		[6] (79, 10, 34)	
			obs.-calc.	obs.-calc.	obs.-calc.	obs.-calc.	obs.-calc.	obs.-calc.	obs.-calc.	obs.-calc.	obs.-calc.	
7	+1	8.5, 7.5	29 251.573	-0.010	28 673.177	0.010	28 127.639	0.000	29 313.664	-0.028	28 179.379	-0.001
	+1	6.5, 5.5	29 253.787	-0.038	28 675.395	0.006	28 129.837	-0.003	29 315.877	-0.058	28 181.585	0.001
	0	8.5	29 342.434	0.035								
	0	7.5	29 235.471	0.169								
	0	6.5	29 163.929	-0.079								
8	+1	9.5, 8.5	32 908.183	-0.012	32 257.516	0.006	31 643.767	-0.003	32 978.052	-0.002	31 702.977	0.000
	+1	7.5, 6.5	32 909.912	-0.036	32 259.242	0.006	31 645.494	0.003	32 979.774	-0.032	31 703.697	-0.003
	0	9.5	32 999.040	-0.042								
	0	8.5	32 893.840	0.146								
	0	7.5	32 819.993	-0.068								
9	+1	10.5, 9.5	36 564.731	0.001	35 841.766	0.005	35 159.835	0.005	32 888.880	-0.064	35 224.505	0.003
	+1	8.5, 7.5	36 566.115	-0.024	35 843.145	-0.003	35 161.214	0.001	36 642.357	0.025	35 225.890	0.003
	0	10.5	36 655.572	-0.045								
	0	9.5	36 551.753	0.125								
	0	8.5	36 475.200	-0.052								
10	+1	11.5, 10.5	39 426.949	0.000	39 426.949	0.000	38 675.825	-0.003			38 746.965	0.000
	+1	9.5, 8.5	39 427.085	-0.004	39 427.085	-0.004	38 676.963	-0.001			38 748.100	-0.003
7	+1	8.5, 7.5	29 016.452	-0.004	28 439.055	0.010	27 894.406	0.004	29 080.350	0.009	27 947.794	0.003
	+1	6.5, 5.5	29 018.301	-0.028	28 440.800	0.000	27 376.258	0.003	29 082.200	-0.014	27 949.655	-0.006
8	0	8.5	29 092.352	-0.025								
	0	7.5	29 002.989	0.119								
	0	6.5	28 942.356	-0.053								
	+1	9.5, 8.5	32 643.637	-0.002	31 994.066	0.002	31 381.340	0.001	29 006.280	-0.024	31 441.395	-0.011
	+1	7.5, 6.5	32 645.077	-0.026	31 995.509	-0.005	31 382.787	0.000	32 716.969	-0.010	31 442.872	0.004
9	0	9.5	32 719.530	-0.030								
	0	8.5	32 631.620	0.103								
	0	7.5	32 569.132	-0.050								
	+1	10.5, 9.5	36 270.752	0.000	35 549.002	-0.018	34 868.203	-0.008	36 350.625	0.002	34 934.967	0.010
	+1	8.5, 7.5	36 271.910	-0.019	35 550.186	0.001	34 869.365	-0.010	36 351.783	-0.016	34 936.139	0.007
10	0	10.5	36 346.639	-0.034								
	0	9.5	36 259.894	0.087								
	0	8.5	36 195.965	-0.043								
	+1	11.5, 10.5	39 897.806	0.002	39 103.924	0.003	38 355.029	0.002	36 275.859	-0.035	38 428.450	-0.004
	+1	9.5, 8.5	39 898.768	-0.003	39 104.886	0.008	38 355.991	0.008	39 985.663	-0.008	38 429.415	-0.004
10	0	11.5	39 973.694	-0.031								
	0	10.5	39 877.903	0.077								
0	9.5	39 822.812	-0.038									
10	0	9.5	39 975.757	0.063								
	0	8.5	39 910.694	-0.034								

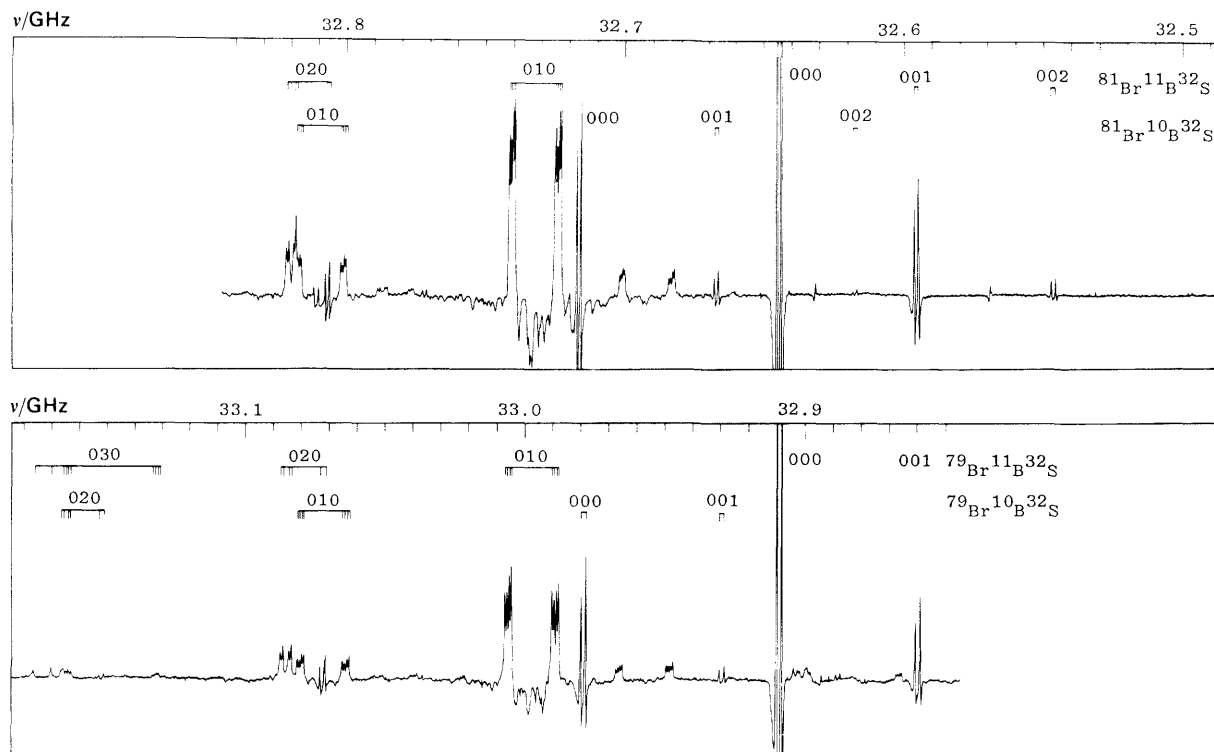


Fig. 1 Medium-resolution scan of the $J = 9 \leftarrow 8$ transition of BrBS

All the transitions exhibit quadrupole splittings due to Br which has a nuclear spin of $I = 3/2$. Ground-state transitions have two strong $\Delta F = +1$ components, and weaker $\Delta F = 0$ components. These are indicated on Fig. 1.

The measured ground-state frequencies and their assignments are given in Table 1. To clarify the presentation of tables, each isotope has been assigned an identification number, $[n]$, as indicated in this table. These data were analysed using the standard formula,¹¹ including quartic centrifugal distortion and first-order interaction for a single quadrupolar nucleus. No splittings due to the ^{10}B , ^{11}B , or ^{33}S nuclei were resolved. The parameters resulting from a least-squares fit of the data to this formula are reported in Table 2, along with the relative abundances of the isotopic species. Few transitions could be reliably identified for the scarce species $^{79}\text{Br}^{10}\text{B}^{33}\text{S}$ [5] or $^{81}\text{Br}^{10}\text{B}^{33}\text{S}$ [11], so molecular parameters are not reported for these molecules.

Structure Determination

Rotational constants of 10 of the 12 possible naturally occurring isotopic modifications of BrBS have been determined, and this large data set allows the calculation of an accurate substitution structure for this molecule. Substitution coordinates obtained by the Kraitchman–Costain method¹⁴ are given in Table 3, where several independent routes have been used to determine a particular atomic coordinate. Evaluation of the coordinates of each atom in the molecule leads to a consistent set of structural data; $r_s(\text{BrB}) = 1.831(2)$ Å, $r_s(\text{B=S}) = 1.608(2)$ Å and $r_s(\text{BrS}) = 3.440(1)$ Å. The quoted Costain errors ($\delta r_s \approx 0.0012/r_s$ ¹⁵) effectively limit the accuracy of the determination, a higher accuracy is implied by the range of values determined for a particular bond length. The main contribution to the Costain error in the bond lengths can be attributed to the boron-atom r_s coordinate, which lies 0.7 Å from the centre of mass.

It is possible to calculate the bond lengths directly, without recourse to centre-of-mass coordinates, by using a method analogous to the Pierce double-substitution procedure.^{11,16} The double-substitution bond length, r_{ss} , is determined from

$$\Delta m_1 \Delta m_2 r_{ss}^2 = MI - M_1^* I_1^* - M_2^* I_2^* + M_{12}^{**} I_{12}^{**}$$

where M and I are the total mass and moment of inertia, respectively, of the parent molecule, subscripts refer to species substituted at the number positions and Δm_i is the change in mass on substituting the i th atom. The number of asterisks indicates the number of substitutions.

The results obtained from this formula are presented in Table 4, where it can be seen that $r_{ss}(\text{BrS})$ is better determined than either $r_{ss}(\text{BrB})$ or $r_{ss}(\text{BS})$, but the range of values obtained is greater than the corresponding range of r_s values.

It is also possible to locate the position of the boron atom from the substitution coordinates of Br and S, and using either the first or second moment equations to give $r_f(\text{B})$ and $r_{ff}(\text{B})$. These values are shown in Table 5, together with $r_s(\text{B})$ for comparison. It can be seen that the values for $r_f(\text{B})$ are consistently higher than the $r_s(\text{B})$ values, and that the $r_{ff}(\text{B})$ coordinates are considerably larger than both. This last effect was also noted for CIBS,¹¹ and is due to the r_s coordinate not reproducing I_0 , but a different value, I_s . This leads to a shift in the boron-atom coordinate when the second moment condition is satisfied. The difference between $r_s(\text{B})$ and $r_{ff}(\text{B})$ coordinates is not as pronounced as in the case of CIBS, because in the case of CIBS the boron atom is very close to the centre of mass of the molecule (*ca.* 0.1 Å).

Structural parameters can be derived using $r_s(\text{Br})$, $r_f(\text{B})$ and $r_s(\text{S})$, and these are given in Table 6. The consistently larger value of $r_f(\text{B})$ than $r_s(\text{B})$ leads to the BrB bond length in this table being consistently longer than $r_s(\text{BrB})$, and a consequent shortening of the B=S bond length relative to $r_s(\text{B=S})$. The range of values in this table is greater than that in Table 3, hence the substitution structure is the preferred structure for this molecule.

Table 2 Ground-state spectroscopic parameters for BrBS

n^a	Br	B	S	B_0/MHz	D_0/Hz	$(eQq)_0/\text{MHz}$	relative abundance (%)
1	79	11	32	1828.2979 (51) ^b	166 (29)	363.55 (9)	100
2	79	11	33	1792.1445 (4)	143 (2)	358.15 (72)	0.79
3	79	11	34	1758.0471 (2)	139 (1)	356.88 (41)	4.44
4	79	10	32	1832.1831 (64)	191 (38)	363.45 (13)	24.39
5	79	10	33	—	—	—	0.18
6	79	10	34	1761.2814 (2)	143 (1)	357.23 (29)	1.04
7	81	11	32	1813.5928 (22)	158 (11)	303.68 (6)	97.94
8	81	11	33	1777.5010 (6)	133 (3)	300.71 (1.11)	0.78
9	81	11	34	1743.4612 (4)	137 (2)	300.43 (76)	4.34
10	81	10	32	1817.5843 (22)	148 (11)	303.64 (6)	22.94
11	81	10	33	—	—	—	0.18
12	81	10	34	1746.7978 (5)	132 (3)	303.23 (90)	1.01

^a Identification number. ^b Errors are one standard deviation in the units of the least-significant digit.

Table 3 Substitution coordinates and bond lengths (Å) for BrBS

a	b	c	d	e	$r_s(\text{Br})$	$r_s(\text{B})$	$r_s(\text{S})$	$r_s(\text{S})$	$r_s(\text{Br—B})^f$	$r_s(\text{B=S})$	$r_s(\text{B=S})^g$	$r_s(\text{Br—S})$	$r_s(\text{Br—S})^h$
1	7	4	2	3	1.067 72	0.763 92	2.371 76	2.371 72	1.831 64	1.607 84	1.607 80	3.439 48	3.439 44
2	8	5	1	3	1.087 05	—	2.352 49	2.352 38	—	—	—	3.439 54	3.429 43
3	9	6	2	1	1.105 95	0.724 95	2.333 47	2.333 52	1.830 90	1.608 52	1.608 57	3.439 42	3.439 47
4	10	1	5	6	1.061 65	0.770 21	—	2.378 14	1.831 86	—	1.607 93	—	3.439 79
6	12	3	5	4	1.100 07	0.730 83	—	2.339 52	1.830 90	—	1.608 69	—	3.439 59
7	1	10	8	9	1.050 50	0.780 55	2.389 03	2.388 95	1.831 05	1.608 45	1.608 40	3.439 53	3.439 45
8	2	11	7	9	1.069 66	—	2.369 91	2.369 75	—	—	—	3.439 57	3.439 41
9	3	12	8	7	1.088 40	0.742 51	2.351 00	2.351 08	1.830 91	1.608 49	1.608 57	3.439 40	3.439 48
10	4	7	11	12	1.044 39	0.786 88	—	2.395 30	—	—	1.608 42	—	3.439 69
12	6	9	10	11	1.084 27	0.748 43	2.357 03	—	1.830 90	1.608 60	—	3.439 50	—

^a Parent. ^b Br substitution. ^c B substitution. ^d First S substitution. ^e Second S substitution. ^f Average = 1.831 17, range = 0.000 96. ^g Average = 1.608 36, range = 0.000 89. ^h Average = 3.439 51, range = 0.000 39.

Table 4 Double-substitution parameters (Å)

	$r_{ss}(\text{Br—B})$		$r_{ss}(\text{B=S})$		$r_{ss}(\text{BrS})$
1a	1.8174	1b	1.5880	1c	3.4383
3a	1.8309	7b	1.6034	1d	3.4385
				2c	3.4387
				4d	3.4350

Each double-substitution distance is preceded by the parent species number and a letter which indicates which other species were used according to: (a) n , $n + 3$, $n + 6$, $n + 9$, (b) n , $n + 2$, $n + 3$, $n + 5$; (c) n , $n + 1$, $n + 6$, $n + 7$; (d) n , $n + 2$, $n + 6$, $n + 8$.

Table 6 Structural parameters (Å) from $r_s(\text{Br})$, $r_s(\text{B})$ and $r_s(\text{S})$

parent	$r(\text{Br—B})$	$r(\text{B=S})$	$r(\text{B=S})$
1	1.8337	1.6058	1.6057
2	1.8341	1.6054	1.6053
3	1.8340	1.6054	1.6054
4	1.8356	—	1.6042
6	1.8338	—	1.6058
7	1.8336	1.6059	1.6058
8	1.8341	1.6055	1.6053
9	1.8341	1.6053	1.6054
10	1.8359	—	1.6038
12	1.8505	1.5908	—
average	1.8360 ± 0.0084	1.6044 ± 0.0075	

Table 5 Boron coordinate data (Å)

parent	r_s	r_I^a	r_{II}^b
1	0.763 92	0.766 01	0.774 88
2	—	0.747 08	0.755 52
3	0.724 95	0.728 09	0.737 21
4	0.770 21	0.773 96	0.778 75
6	0.730 83	0.733 77	0.742 73
7	0.780 55	0.783 12	0.791 66
8	—	0.764 46	0.772 73
9	0.742 51	0.745 69	0.754 65
10	0.786 88	0.791 53	0.796 88
12	0.748 43	0.766 19	0.740 07

^a First moment position using $r_s(\text{Br})$ and the average value of $r_s(\text{S})$.

^b Second moment position using $I_0(n)$, $r_s(\text{Br})$ and the average value of $r_s(\text{S})$.

Vibrational Analysis

Spectra due to molecules in various vibrationally excited states have been observed. An analysis has been carried out for various isotopic modifications of BrBS with up to three quanta of the degenerate bending mode ν_2 excited (Tables 7–9), and up to two quanta of the stretch ν_3 (Table 10). The quantum number l , associated with vibrationally induced angular momentum about the figure axis, could be deduced by the quadrupole structure and the Stark effect of each group of lines. Transitions for which $l = 0$ behave like ground state lines, *i.e.* they consist of two very strong components and have slow-second-order Stark effects so are not strongly modulated at low electric field strengths. Transitions for

Table 7 Transition frequencies and assignments for the (010) vibrational satellites

<i>J</i>	<i>l</i>	<i>F</i> "	[1]	obs.–calc.	[4]	obs.–calc.	[7]	obs.–calc.	[10]	obs.–calc.
7	+1	8.5	29 337.197	0.017	29 403.275	0.055	29 101.413	0.000	29 169.253	0.069
		7.5	29 338.256	0.005	29 404.338	0.052	29 102.300	0.000	29 170.138	0.059
		6.5	29 340.123	–0.036	29 406.200	0.013	29 103.859	–0.022	29 171.650	–0.023
		5.5	29 339.052	–0.036	29 405.110	–0.011	29 102.958	–0.036	29 170.773	–0.006
7	–1	8.5	29 322.217	–0.019	29 388.796	0.062	29 086.660	–0.008	29 154.998	0.081
		7.5	29 323.275	–0.031	29 389.842	0.042	29 087.544	–0.010	29 155.899	0.087
		6.5	29 325.192	–0.023	29 391.768	0.066	29 089.142	0.007	29 157.476	0.070
		5.5	29 324.113	–0.031	29 390.670	0.035	29 088.242	–0.006	29 156.221	0.088
8	+1	9.5	33 004.670	0.016	33 079.028	0.067	32 739.358	0.011	32 815.675	0.040
		8.5	33 005.413	0.010	33 079.750	0.042	32 739.963	–0.005	32 816.278	0.016
		7.5	33 006.922	–0.024	33 081.250	0.006	32 741.226	–0.019	32 817.566	0.016
		6.5	33 006.169	–0.027	33 080.495	–0.003	32 740.609	–0.016	32 816.928	0.004
8	–1	9.5	32 987.823	–0.019	33 062.730	0.065	32 722.750	–0.008	32 799.642	0.057
		8.5	32 988.567	0.010	33 063.479	0.068	32 723.360	–0.019	32 800.243	0.039
		7.5	32 990.110	–0.024	33 065.017	0.069	32 724.651	–0.005	32 801.545	0.045
		6.5	32 989.355	–0.029	33 064.262	0.061	32 724.032	–0.004	32 800.925	0.051
9	+1	10.5	36 672.050	0.038	36 754.632	0.039	36 377.178	–0.003	36 461.973	–0.028
		9.5	36 672.568	0.011	36 755.157	0.021	36 377.628	–0.004	36 462.422	–0.034
		8.5	36 673.810	–0.016	36 756.387	–0.013	36 378.667	–0.016	36 463.462	–0.054
		7.5	36 673.283	0.002	36 755.856	–0.001	36 378.203	–0.029	36 463.030	–0.031
9	–1	10.5	36 653.305	–0.027	36 736.547	0.062	36 358.737	–0.012	36 444.173	0.006
		9.5	36 653.836	–0.041	36 737.078	0.050	36 359.183	–0.017	36 444.619	–0.004
		8.5	36 655.094	–0.052	36 738.348	0.056	36 360.247	–0.004	36 445.783	0.100
		7.5	36 654.569	–0.032	36 737.807	0.058	36 359.786	–0.014	36 445.230	0.003
10	+1	11.5					40 014.940	0.006		
		10.5					40 015.271	–0.001		
		9.5					40 016.138	–0.013		
		8.5					40 015.802	–0.010		
10	–1	11.5					39 994.650	–0.008		
		10.5					39 994.982	–0.015		
		9.5					39 995.857	–0.018		
		8.5					39 995.532	–0.005		

Table 8 Transition frequencies and assignments for the (020) vibrational satellites

<i>J</i>	<i> l </i>	<i>F</i> "	[1]	obs.–calc.	[4]	obs.–calc.	[7]	obs.–calc.	[10]	obs.–calc.
7	0	8.5, 7.5	29 396.583				29 160.450		29 234.778	
		6.5, 5.5	29 398.756				29 162.282		29 235.491	
7	2	8.5	29 406.854	–0.001	29 477.412	0.011	29 170.768	0.005	29 243.045	0.081
		7.5	29 411.072	–0.021	29 481.685	0.079	29 174.288	0.046	29 246.612	0.107
		6.5	29 412.066	0.006	29 482.530	–0.035	29 175.082	0.046	29 247.395	0.082
		5.5	29 407.772	–0.050	29 478.322	–0.038	29 171.660	0.103	29 243.728	–0.044
8	0	9.5, 8.5	33 071.320				32 805.638		32 887.201	
		7.5, 6.5	33 073.015				32 807.055		32 888.610	
8	2	9.5	33 083.516	–0.005	33 162.873	–0.049	32 817.744	–0.014	32 898.998	–0.079
		8.5	33 086.474	–0.013	33 165.818	–0.048	32 820.240	0.047	32 901.548	–0.008
		7.5	33 087.444	0.000	33 166.791	–0.024	32 821.050	0.072	32 902.260	–0.095
		6.5	33 084.446	–0.032	33 163.812	–0.059	32 818.520	–0.023	32 899.820	–0.056
9	0	10.5, 9.5	36 745.984				36 450.750			
		8.5, 7.5	36 747.345				36 451.890			
9	2	10.5	36 759.947	–0.012	36 848.146	–0.086	36 464.558	–0.002		
		9.5	36 762.099	–0.017	36 850.290	–0.083	36 466.360	0.029	36 556.720	–0.105
		8.5	36 762.979	–0.021	36 851.142	–0.108	36 467.110	0.053	36 557.452	–0.112
		7.5	36 760.800	–0.043	36 849.083	–0.026	36 465.260	–0.026		

which $l \geq 1$ have larger quadrupole splittings, different hyperfine intensity patterns and fast first-order Stark effects. In the case of $|l| = 1$, the lines are resolved into four components, and are modulated at *ca.* 50 V cm^{–1}. The quantum number v_2 was assigned on the basis of relative intensity and displacement from the ground-state lines.

The analysis of the degenerate bending mode satellites was carried out using a standard formula¹⁷ involving the ground-state rotational constant and its variation with vibrational quantum number, the ground-state quartic centrifugal distortion constant and the vibration–rotation interaction constants γ_{22} and γ_{ll} . The large l -doubling splitting, which occurs for $|l| = 1$, is described by q_2 . The effects of the quadrupolar

bromine nuclei were accounted for by introducing the first-order correction term of Tarrago and Maes,¹⁷ which allows the vibrational dependence of the hyperfine splitting to be determined *via* the parameter α_2^{eQq} .

The use of this formula is restricted to states for which $v_2 = |l|$; other states are subject to Fermi resonance, similar to that seen in CIBS.¹¹ This can be seen from Fig. 1. The l -doublets of the (030) state are shifted to low frequency, and are not symmetrically disposed about the $|l| = 3$ components, as would be expected. This is due to the interaction between the (03¹0) and (01¹1) states. Also, the (02²0) and (02⁰0) transitions are anomalously far apart. This separation is expected to be *ca.* 1–2 MHz in the absence of resonance,

Table 9 Frequencies and assignments for the (030) vibrational satellites

<i>J</i>	<i>l</i>	<i>F</i> ^o	[1]	obs.-calc.	[7]	obs.-calc.
7	3	8.5	29 483.032	-0.019	29 246.600	-0.062
		7.5	29 492.458	-0.026	29 254.102	-0.235
		6.5	29 491.982	0.061	29 253.645	-0.234
		5.5	29 482.554	0.066	29 246.158	-0.046
7	-1	8.5			29 213.390	
		7.5			29 214.374	
		6.5			29 215.948	
		5.5			29 214.983	
8	3	9.5, 6.5	33 170.001	-0.033	32 903.781	-0.004
		8.5, 7.5	33 176.628	-0.009	32 909.337	0.179
8	+1	9.5	33 164.061		32 865.325	
		8.5	33 166.263		32 864.773	
		7.5	33 165.533		32 866.596	
		6.5	33 165.533		32 866.596	
8	-1	9.5	33 131.192		32 865.301	
		8.5	33 131.941		32 865.950	
		7.5			32 867.211	
		6.5	33 133.479		32 866.599	
9	3	10.5, 7.5	36 856.690	0.087	36 560.646	-0.021
		9.5, 8.5	36 861.490	0.085	36 564.620	0.045
9	+1	10.5	36 848.134			
		9.5	36 849.101			
		8.5	36 851.169			
		7.5	36 850.302			
9	-1	10.5	36 812.640		36 517.150	
		9.5	36 813.261		36 517.596	
		8.5	26 814.425		36 518.752	
		7.5	36 813.891		36 518.196	

Table 10 Frequencies and assignments of the (001) and (002) vibrational satellites

<i>J</i>	<i>v</i>	<i>F</i> ^o	[1]	obs.-calc.	[4]	obs.-calc.	[7]	obs.-calc.
7	1	8.5, 7.5	29 207.710	-0.015	29 269.465	-0.013	28 972.972	-0.011
		6.5, 5.5	29 209.928	-0.033	29 271.676	-0.044	28 974.842	-0.088
8	1	9.5, 8.5	32 858.842	-0.013	32 928.313	0.001	32 594.730	-0.001
		7.5, 6.5	32 860.575	-0.028	32 930.043	-0.021	32 596.179	-0.012
9	1	10.5, 9.5	36 509.900	-0.007	36 587.098	0.036	36 216.424	0.014
		8.5, 7.5	36 511.295	-0.017	36 588.497	0.027	36 217.577	-0.006
10	1	11.5, 10.5					39 838.040	0.012
		9.5, 8.5					39 838.996	0.005
7	2	8.5, 7.5	29 163.880	0.012				
		6.5, 5.5	29 166.085	-0.013				
8	2	9.5, 8.5	32 809.512	-0.003			32 545.803	-0.021
		7.5, 6.5	32 811.275	0.018				
9	2	10.5, 9.5	35 455.105	0.021			36 162.062	-0.006
		8.5, 7.5	36 456.500	0.015			36 163.235	-0.002
10	2	11.5, 10.5					39 778.270	0.019
		9.5, 8.5					39 779.217	0.006

Table 11 Vibration-rotation parameters

	α_2 /MHz	α_2^{0q} /MHz	q_2 /MHz	γ_{22} /kHz	α_3 /MHz
[1]	-4.9266 (11) ^a	3.80 (32)	0.9340 (62)	-6.71 (25)	2.7412 (13)
[4]	-5.1678 (35)	5.1 (1.2)	0.9054 (89)	-2.30 (78)	2.7635 (10)
[7]	-4.8894 (12)	5.71 (45)	0.9216 (9)	-6.72 (26)	2.7172 (3)
[10]	-5.1324 (29)	3.0 (1.3)	0.8917 (87)	-4.14 (78)	—

^a Errors in brackets are one standard deviation.

but is observed to be 12 MHz. This is a consequence of the interaction between the (02⁰0) and (001) states. Rovibrational constants for these states are given in Table 11. It is not possible to separate the effects of γ_{22} and γ_{11} using only $v_2 = l$ lines, so their sum is given. It has been found that for the substitution ¹¹B → ¹⁰B, α_2 increases by ca. 0.3 MHz, whereas the result of ⁸¹Br → ⁷⁹Br substitution is an increase of only ca. 0.03 MHz. These shifts are independent of the isotopic configuration. The change in q_2 for the above substitutions are similar in magnitude (ca. 0.01 MHz), but the changes for

boron are in the opposite sense compared with that of bromine. These trends are similar to those observed for CIBS,¹¹ although slightly smaller.

An approximate bending vibrational frequency can be calculated from¹⁸

$$\omega_2 \approx fB_0^2/q_2; \quad f = 2-2.6$$

Using this formula, a similar situation was found to that of CIBS,¹¹ i.e. for molecules with the same mass boron atom, the changes in B_0 and q_2 compensate to give identical

bending frequencies. Thus for all ^{11}B species we find $\omega_2 \approx 270 \pm 40 \text{ cm}^{-1}$, and for all ^{10}B species $\omega_2 \approx 280 \pm 40 \text{ cm}^{-1}$. An estimate for the Br—B stretching frequency, ω_3 can be made from the relative intensities of the (001) and (002) transitions. For $^{79}\text{Br}^{11}\text{B}^{32}\text{S}$ we find $\omega_3 \approx 414 \pm 14 \text{ cm}^{-1}$.

Discussion

A detailed analysis of the rotational spectrum of BrBS has been presented, and has yielded information on the geometric structure, the quadrupole coupling constants, the vibration-rotation parameters and some of the vibrational frequencies of the molecule. There is now much information on the structure of the sulphidoboron series, and many of the salient parameters are collected in Table 12, together with nitrile data for comparison. The B=S bond length is consistent down the series, as might be expected, a consistency which is mirrored in the analogous nitrile series.

The degree of π -bonding between the bromine and boron atoms can be estimated from the $(eQq)_0$ values given in Table 2.¹⁹ Using the values 2.8 and 2.0¹⁹ for the electronegativities of bromine and boron, respectively, gives a sigma bond ionic character $i_\sigma = 0.4$. Use of the value $eQq_{n10}(^{79}\text{Br}) = -769.76$

Table 12 Structural data (Å) for XB=S and XC≡N species^a

X	$r(\text{X}-\text{B})$	$r(\text{B}=\text{S})$	$r(\text{X}-\text{C})^b$	$r(\text{C}=\text{N})^b$
H		1.5995	1.0659 ^c	1.155 ^c
CH ₃	1.5352 ^d	1.6028 ^d	1.458	1.157
F	1.284 ^{e, f}	1.606 ^f	1.262	1.159
Cl	1.681 ^g	1.606 ^g	1.629 ^c	1.160 ^c
Br	1.831 ^h	1.608 ^h	1.789	1.160

^a r_s values unless otherwise stated. ^b From ref. 19. ^c r_e value. ^d From ref. 10. ^e r_1 value. ^f From ref. 13. ^g From ref. 11. ^h This work.

MHz¹⁹ results in a π -bond character $\pi_c = 0.255$, and a resultant ionic character of $i_c = 0.145$. The value of π_c is similar to that found in CIBS¹¹ (0.225), although the resultant ionic character is lower (0.275 in the case of CIBS).

References

- 1 R. W. Kirk and P. L. Timms, *J. Chem. Soc., Chem. Commun.*, 1967, 18.
- 2 E. F. Pearson and R. V. McCormick *J. Chem. Phys.*, 1973, **58**, 1619.
- 3 E. F. Pearson, C. L. Norris and W. H. Flygare, *J. Chem. Phys.*, 1974, **60**, 1761.
- 4 H. W. Kroto, R. J. Suffolk and N. P. C. Westwood, *Chem. Phys. Lett.*, 1973, **22**, 495.
- 5 T. P. Fehlner and D. W. Turner, *J. Am. Chem. Soc.*, 1973, **95**, 7175.
- 6 R. L. Sams and A. G. Maki, *J. Mol. Struct.*, 1975, **26**, 107.
- 7 P. H. Turner and I. M. Mills, Seventh Colloquium on High Resolution Spectroscopy, 1981, Reading, Paper L15.
- 8 H. W. Kroto, *Chem. Soc. Rev.*, 1982, **11**, 435.
- 9 C. Kirby, H. W. Kroto and M. J. Taylor, *J. Chem. Soc. Chem. Commun.*, 1978, 19.
- 10 C. Kirby and H. W. Kroto, *J. Mol. Spectrosc.*, 1980, **83**, 1.
- 11 C. Kirby and H. W. Kroto, *J. Mol. Spectrosc.*, 1980, **83**, 130.
- 12 C. Kirby, H. W. Kroto and N. P. C. Westwood, *J. Am. Chem. Soc.*, 1978, **100**, 3766.
- 13 T. A. Cooper, *Ph.D. Thesis*, University of Sussex, 1981.
- 14 C. C. Costain, *J. Chem. Phys.*, 1958, **29**, 864.
- 15 C. C. Costain, *Trans. Am. Crystallogr. Soc.*, 1966, **2**, 157.
- 16 L. Pierce, *J. Mol. Spectrosc.*, 1958, **3**, 575.
- 17 G. Tarrago and S. Maes, *C. R. Acad. Sci. Paris Ser. B*, 1968, **266**, 699.
- 18 C. H. Townes and A. L. Schawlow, *Microwave Spectroscopy*, McGraw-Hill, New York, 1955.
- 19 W. Gordy and R. L. Cook, *Microwave Molecular Spectra*, Wiley, New York, 1974.

Paper 0/03671D; Received 9th September, 1990